Heat capacity proportional to T^2 induced by Ru substitution in $CaCu_3(Ti_{4-x}Ru_x)O_{12}$ ($x \approx 0.5$)

I. Tsukada,[1,*] R. Kammuri,[2] T. Kida,[2] S. Yoshii,[2] T. Takeuchi,[3] M. Hagiwara,[2] M. Iwakawa,[4] W. Kobayashi,[4] and I. Terasaki[4]
[1]*Central Research Institute of Electric Power Industry, Tokyo 201-8511, Japan*
[2]*KYOKUGEN, Osaka University, Osaka 560-8531, Japan*
[3]*Low Temperature Center, Osaka University, Osaka 560-8531, Japan*
[4]*Department of Applied Physics, Waseda University, Tokyo 169-6855, Japan*
(Received 4 December 2008; revised manuscript received 19 January 2009; published 26 February 2009)

The effect of Ru substitution for Ti on the ground-state properties of three-dimensional antiferromagnet (AF) $CaCu_3Ti_4O_{12}$ is studied by means of magnetic susceptibility and heat-capacity measurements. A small amount of Ru substituted for Ti suppresses AF long-range order and induces a new intermediate state with T^2-proportional heat capacity, which shows a clear contrast to a simple spin-dilution effect demonstrated by the Zn substitution for Cu. Ru substitution also creates a finite density of state at the Fermi level while keeping nominal valence of Cu ions to be 2+, which is essential to a novel insulator-to-metal crossover driven by an isovalent substitution of Ru^{4+} for Ti^{4+}.

DOI: 10.1103/PhysRevB.79.054430 PACS number(s): 75.40.−s, 71.30.+h, 71.28.+d, 75.10.Nr

I. INTRODUCTION

Competition of the two different ground states can create a new state that cannot be understood as a simple mixture of the two end states. The solid solution of $CaCu_3(Ti_{4-x}Ru_x)O_{12}$ is an interesting compound from this viewpoint because it spans a gap between two contrasting novel properties.[1,2] It shows a three-dimensional (3D) antiferromagnetic long-range order (AF-LRO) with a huge dielectric constant at one end ($x=0$) (Refs. 3–6) while it goes into a novel valence-fluctuating state at the other end ($x=4$),[1,2] which is also supported by the recent comprehensive study including NMR and nuclear quadrupole resonance (NQR) results.[7] Recent research on the Ru-substitution effect in $CaCu_3Ti_4O_{12}$ by Kobayashi *et al.*[1] suggested the creation of a new state at intermediate x. They found that electrical resistivity decreased gradually toward $x=1.5$, while thermopower decreased rapidly to a few μV K^{-1} already at $x=1.0$. Magnetic susceptibility showed a smooth decrease of Néel temperature (T_N), Curie constant (C_{Curie}), and Weiss temperature (θ_W), while smooth increase was observed in Pauli's paramagnetic contribution (χ_p), which is not understood as a consequence of the simple blend of insulator and metal.

In this paper, we revisit the magnetic susceptibility to see how the antiferromagnetic long-range order of $CaCu_3Ti_4O_{12}$ collapses upon Ru substitution for Ti. We find that the magnetic ground state sensitively changes its character with x. A 3D AF-LRO at $x=0$ is completely replaced by a new state at $x=0.5$, followed by a spin-glass (SG) -like state at $1.0 \leq x \leq 1.5$. In order to clarify a thermodynamic property of these states, we measure heat capacity for the representative compositions. We also compare Ru substitution for Ti with Zn substitution for Cu because the latter substitution is considered to simply dilute spins without carrier doping.

II. EXPERIMENTAL DETAILS

We used six sintered pellets of $CaCu_3(Ti_{4-x}Ru_x)O_{12}$ ($x=0$, 0.5, 1.0, 1.3, 1.5, and 4.0), part of which were previously characterized with electrical resistivity, thermopower, and magnetic susceptibility.[1] The x-ray diffraction (not shown) of the Ru-substituted sample is quite similar to that of the parent $x=0$ compounds, which supports the absence of apparent impurities. We also confirm that peak widths of the 422 reflection of mixed compounds ($x=0.5 \sim 1.5$) are almost identical to that of $x=0$, which reasonably excludes a possible inhomogeneity in the mixed compounds. For the heat-capacity measurements, we selected four compositions with $x=0$, 0.5, 1.5, and 4.0. Each pellet was cut into a rectangular shape with a typical weight of 10–20 mg. We also tried to synthesize three $Ca(Cu_{3-z}Zn_z)Ti_4O_{12}$ ($z=0.5$, 1.0, and 1.5) polycrystalline samples, but we could successfully obtain $z=0.5$ only. dc magnetic susceptibility was measured by a commercial superconducting quantum interference device (SQUID) magnetometer (MPMS, Quantum Design), where we utilized a zero-field option to perform zero-field-cooled (ZFC) measurements. Heat capacity was measured by a conventional relaxation method (PPMS, Quantum Design). In the following sections, we plot magnetic susceptibility in the unit of emu Cu mol^{-1} as a regular rule, except when specially noted, because Curie-Weiss-type behavior can be attributed purely to Cu^{2+} ions. On the other hand, heat capacity is normalized by formula-unit mole in order to discuss the complicated interplay between localized and itinerant electrons.

III. RESULTS

A. Magnetic susceptibility and phase diagram

At the beginning, we measure the magnetic susceptibility $\chi(T)$ of $CaCu_3Ti_4O_{12}$ at $H=100$ Oe [see Fig. 1(a)]. As is noted above, the data are plotted in the unit of emu Cu mol^{-1} in order to trace the change of localization of the electron on each Cu^{2+} ion. Though the data basically reproduce the previous measurements by Kobayashi *et al.*,[1] we find that the low-temperature ordered state is different from the conventional 3D AF-LRO state for $x \geq 0.5$ and its x dependence is much complicated. The data for the $x=4.0$ are completely identical to that in Ref. 1, but slightly larger than that re-

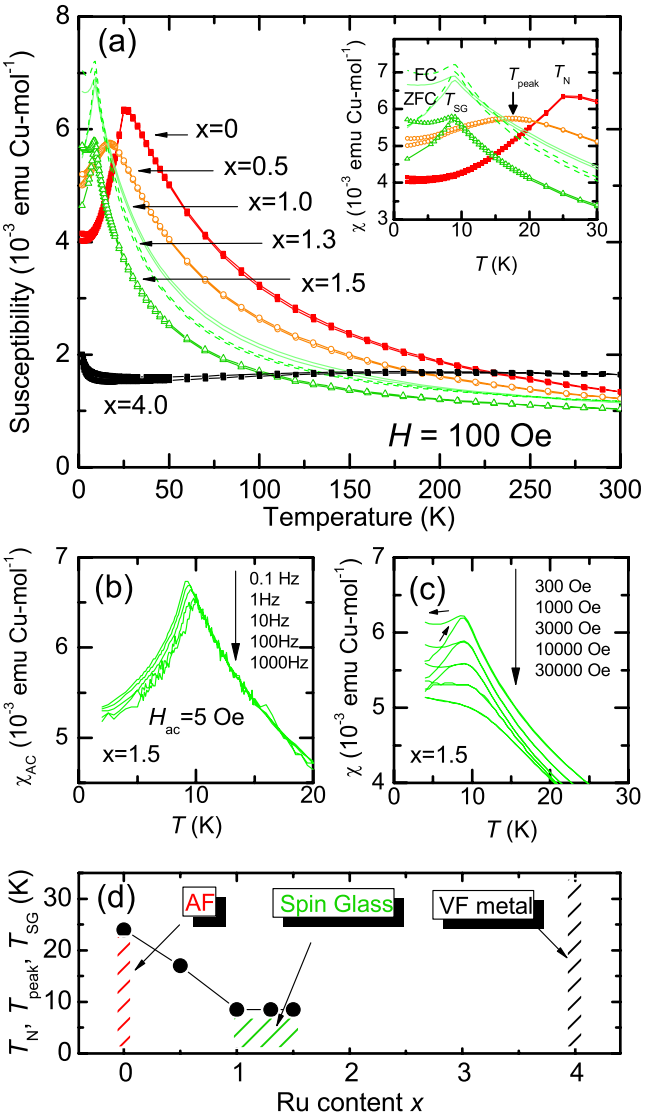

FIG. 1. (Color online) (a) Temperature dependence of the dc magnetic susceptibility of $CaCu_3(Ti_{4-x}Ru_x)O_{12}$ measured at $H=100$ Oe with ZFC and FC processes. Inset shows $\chi(T)$ at $T \leq 30$ K. (b) ac susceptibility for $x=1.5$ at $10^{-1}-10^{3}$ Hz. The amplitude of the ac magnetic field is 5 Oe. (c) $\chi(T)$ for $x=1.5$ at various magnetic fields. (d) The magnetic phase diagram deduced from the susceptibility.

ported in Ref. 7, which might be related to the difference between the magnitude of resistivity of $CaCu_3Ru_4O_{12}$ reported in Refs. 1 and 7.

For the $x=0$, $\chi(T)$ shows a peak around $T=25$ K and almost no hysteresis is observed between ZFC and field-cooled (FC) processes. We determine T_N to be 24 K following to the Fisher's method,[8] according to which T_N is given by the temperature where $\partial[T\chi(T)]/\partial T$ takes a local maximum. This T_N shows good agreement with the peak position of the heat-capacity data as predicted by Fisher.[8] The present estimation of T_N is identical to that reported for a single crystal in Ref. 6. We notice that $\chi(2\text{ K})=4.0\times10^{-3}$ emu Cu mol^{-1} is roughly equal to 2/3 of $\chi(T_N)$ as expected for a powder sample with axial anisotropy. It is also worth noting that the effective moment p_{eff} estimated from C_{Curie} is about $1.95\mu_B$, which is reasonably close to the value expected for $S=1/2$ $(1.73\mu_B)$ and also consistent with the recently reported value $(1.91\mu_B)$.[9] As a result, we can safely conclude that a classical 3D AF-LRO state is realized in $CaCu_3Ti_4O_{12}$.

A small amount of Ru substituted for Ti alters the magnetic ground state of $CaCu_3Ti_4O_{12}$ drastically but not straightforwardly. At $x=0.5$, a sharp peak around T_N is replaced by a broad one as shown in the inset of Fig. 1(a). We define the peak temperature as T_{peak} for convenience, but we can no longer recognize a sharp phase transition at $T_{\text{peak}}=17$ K indicating that the ground state is no longer a 3D AF-LRO state. It should be also noted that the state below T_{peak} is different from a classical SG state because the hysteresis between ZFC and FC processes remains small as for the $x=0$. The hysteresis becomes obvious only after x exceeds 1.0, which automatically means that the $x=0.5$ phase is not a SG state, at least in a classical manner. Thus, this intermediate state at $x=0.5$ should be strictly distinguished from both of the 3D AF-LRO and the SG states.

Finite hysteresis observed for $1.0\leq x\leq1.5$ may suggest that a SG state shows up. For these x's, a sharp cusp is observed in $\chi(T)$ at $T_{\text{SG}}=8.5$ K with finite hysteresis between ZFC and FC processes. The shape of hysteresis looks similar to a classical SG. In order to confirm this assignment, we measure ac susceptibility of $x=1.5$ at various frequency with $H_{\text{ac}}=5$ Oe as shown in Fig. 1(b). By increasing frequency, T_{SG} increases qualitatively consistent with conventional SG materials. However, it should be noted that the frequency dependence of T_{SG} is very weak in comparison to a conventional SG state. With changing the frequency from 0.1 to 1000 Hz, T_{SG} increases only by 11%, which is quite small as for a conventional SG material. Thus, this SG-like state is "hard" to an external field. Figure 1(c) also implies the presence of such hardness. While the dc susceptibility exhibits broadening of the cusp with suppression of T_{SG} suggesting a typical feature of a conventional SG state,[10] its field dependence remains very weak. Therefore, we should assign this phase $(1.0\leq x\leq1.5)$ to be a SG-like state and rigorously distinguish from a classical SG state. It is interesting to see that T_{SG} shows almost no x dependence in this region, suggesting that the spin-spin interaction is insensitive to the amount of Ru as predicted by the mean-field theories of Edwards and Anderson[11] (EA) and Sherrington and Kirkpatrick[12] (SK) models.

Consequently, the magnetic phase diagram is summarized as shown in Fig. 1(d). We can identify, at least, four different states: (1) the 3D AF-LRO state at $x=0$, (2) the intermediate state at $x=0.5$, (3) the SG-like state between $1.0\leq x\leq1.5$, and (4) the valence fluctuating metal state at $x=4.0$. From Sec. III B, we will see heat capacity of these four states to see their differences in more detail.

B. Specific heat

The heat capacity of $CaCu_3(Ti_{4-x}Ru_x)O_{12}$ shown in Fig. 2(a) reinforces the classical nature of 3D AF state at $x=0$. Note that the data are plotted as a value per formula-unit mole. For $CaCu_3Ti_4O_{12}$, we obtained quantitatively the same

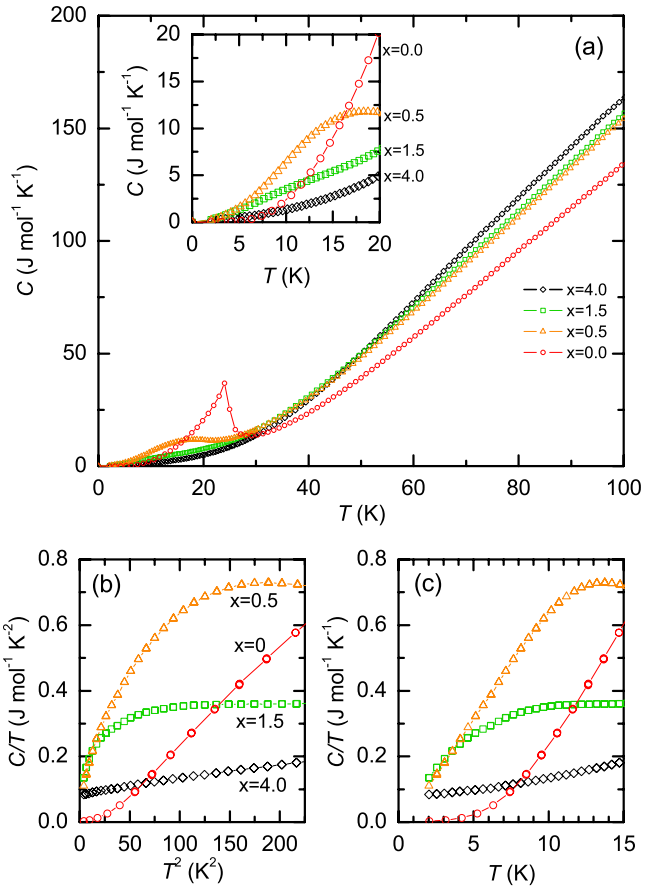

FIG. 2. (Color online) (a) Temperature dependence of the heat capacity of $CaCu_3(Ti_{4-x}Ru_x)O_{12}$ (x=0, 0.5, 1.5, 4.0). Inset shows the same data at the low-temperature region of $T \leq 20$ K. (b) C/T vs T^2 plot and (c) C/T vs T plot for the same set of samples.

result as Ramirez *et al.*[2] The λ-shape anomaly is observed and the peak appears at T=24 K showing a good agreement with T_N determined from magnetic susceptibility. Below T_N, the heat capacity has a form of $C(T) \propto T^3$ except at the very low temperatures [see Fig. 2(b)] indicating that the magnetic contribution to the total heat capacity follows T^3 law as expected from the classical spin-wave theory of antiferromagnets.[13] The data also show that electronic specific-heat coefficient γ=0, which is consistent with insulating nature of $CaCu_3Ti_4O_{12}$.

The sharp transition observed at x=0 is no longer observed at x=0.5. Instead, $C(T)$ exhibits a rounded peak at $T \approx 17$ K indicating a strong correlation to the magnetic susceptibility. What is striking is the temperature dependence of C below 17 K. As can be seen from Fig. 2(b), C/T is not linear to T^2 implying that the total heat capacity is not a simple sum of γT and βT^3 terms as expected for a simply carrier-doped AF compound. This result suggests that spin and electronic excitations in $CaCu_3(Ti_{4-x}Ru_x)O_{12}$ are no longer independent from each other, but strongly correlate to each other. In order to clarify its temperature dependence, we replot C/T as a function of T instead of T^2 in Fig. 2(c). It is surprising for x=0.5 that C/T shows a clear T-linear dependence, i.e., C is proportional to T^2. This T^2-proportional behavior dominates most of all the region below T_{peak}. On the other hand, such a strange temperature dependence cannot be found in the x=1.5 sample at $T>2$ K. The heat capacity looks rather linear to T as shown in the inset of Fig. 2(a). Thus, the T^2-proportional heat capacity is probably characteristic only to the intermediate state around x=0.5.

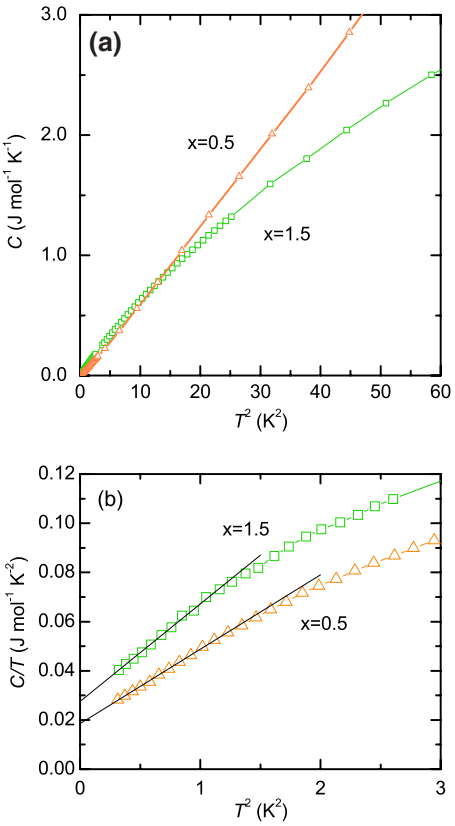

FIG. 3. (Color online) (a) C vs T^2 plot for the x=0.5 and 1.5 samples. (b) C/T vs T^2 plot for the x=0.5 and 1.5 samples measured by ^{3}He refrigerator. Solid lines are linear fit to the lowest part of the data for both the samples.

We further extend measurement range down to 0.5 K and replot $C(T)$ of x=0.5 and 1.5 as functions of T^2 to clarify if there is a qualitative difference between x=0.5 and 1.5. Figure 3(a) indicates that the T^2-proportional behavior is retained roughly in the whole range below 7 K, while for x =1.5 we cannot confirm T^2-proportional behavior at all. Therefore, we should conclude that x=0.5 and 1.5 have different magnetic ground states. Another important finding from the measurements down to 0.5 K is that the T^2-proportional behavior does not hold to the lowest temperature. In Fig. 3(b), we show a C/T vs T^2 plot again for the x=0.5 and 1.5. We see below T=1 K that C/T looks proportional to T^2 and its extrapolation to T=0 K gives finite electronic specific-heat coefficient; γ=0.0185 J mol^{-1} K^{-1} and 0.0275 J mol^{-1} K^{-1} for x=0.5 and 1.5, respectively. This is qualitatively consistent with the evolution of Pauli's paramagnetic susceptibility (χ_p) suggested by $\chi(T)$ and supports the presence of a finite density of state (DOS) at Fermi level. We will discuss it later.

C. Zn substitution for Cu

In order to clarify the peculiarity of the effect of Ru substitution for Ti, it is useful to compare it to Zn (S=0 for

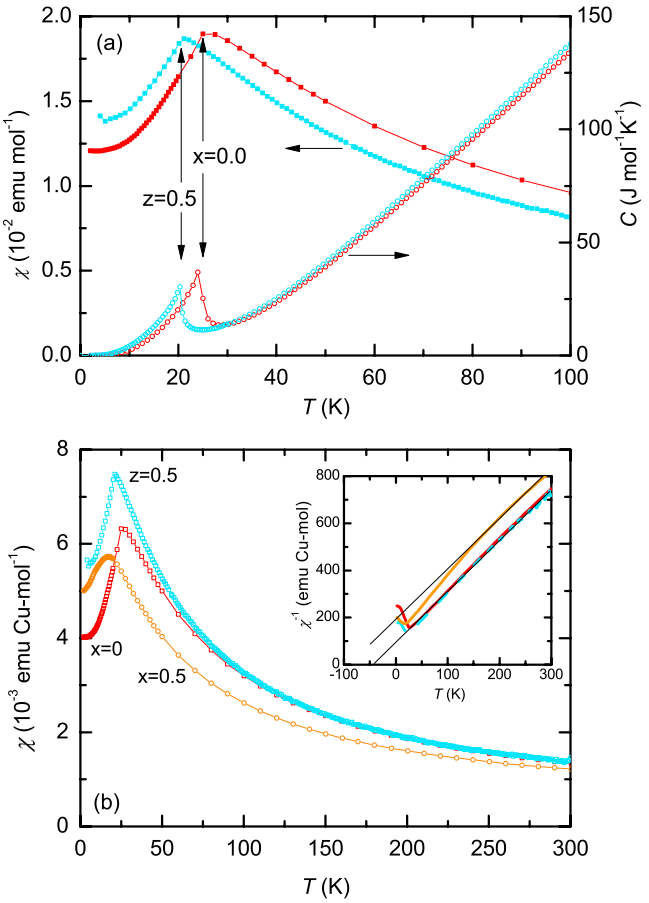

FIG. 4. (Color online) (a) $\chi(T)$ (left axis, filled symbols) and $C(T)$ (right axis, open symbols) for $x=0$ and $z=0.5$. (b) $\chi(T)$ of $x=0$, $z=0.5$, and $x=0.5$ normalized per Cu mol. Inset shows the inverse of $\chi(T)$. For the Ru-free samples, $\chi^{-1}(T)$'s almost look straight, while the deviation from the straight line becomes obvious for $x=0.5$, indicating the evolution of χ_p by Ru substitution.

Zn^{2+}) substitution for Cu ($S=1/2$ for Cu^{2+}) because much simpler suppression of AF-LRO by spin dilution is expected in the latter case. Figure 4(a) shows $\chi(T)$ and $C(T)$ for $z=0.5$ with that for $x=0$ (corresponding to $z=0$). Note that $\chi(T)$ is plotted in the unit of emu mol^{-1} instead of emu Cu mol^{-1} in order to see the decrease of the number of localized spins clearly. T_N is moderately suppressed down to 20 K while keeping sharpness of the transition at T_N, both in $\chi(T)$ and $C(T)$, and more importantly T^2 dependence does not emerge in $C(T)$ indicating that the Zn substitution for Cu merely suppresses 3D AF LRO following a simple dilution effect.[14,15] Next, we replot the susceptibility normalized by Cu mol in Fig. 4(b) in order to evaluate how each spin changes its character by Zn substitution. Then we can easily see that $\chi(T)$ of $z=0.5$ is almost identical to that of $x=0$ at $T>100$ K, while $\chi(T)$ of $x=0.5$ shows an obvious decrease from that of $x=0$. Thus, the magnitude of spin on Cu^{2+} does not change with Zn substitution, which again highlights the strong suppression of the spin by Ru substitution. As is seen in the inset of Fig. 4(b), the inverse susceptibility is well fitted by conventional Curie-Weiss low without assuming the presence of χ_p contribution, consistent with that Zn substitution does not introduce mobile carrier. On the other hand,

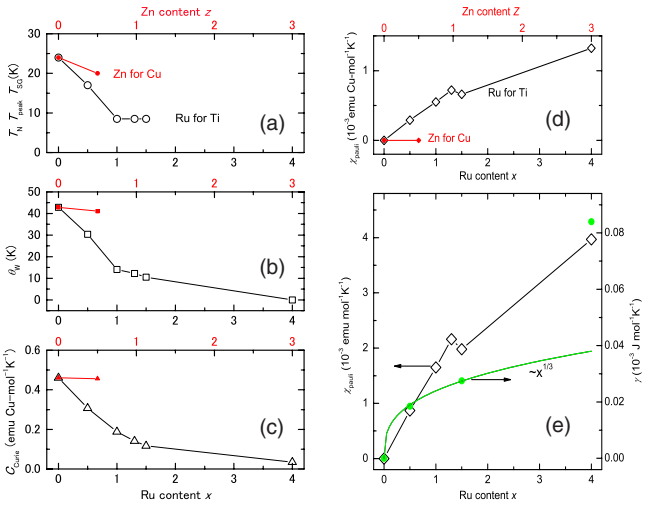

FIG. 5. (Color online) (a)–(d) x or z dependence of T_N (T_{peak},T_{SG}), θ_W, C_{Curie}, and χ_p. Note that C_{Curie} and χ_p is normalized per mol Cu. (e) x dependence of χ_p and γ. All the data are normalized by mol formula unit, thus the χ_p is larger by 3 times than that shown in (d).

$\chi^{-1}(T)$ for $x=0.5$ shows an explicit deviation from the straight line indicating finite contribution from χ_p.

In Figs. 5(a)–5(d), we plot several parameters obtained by fitting the susceptibility in the temperature region of $100 \leq T \leq 250$ K assuming the following formula:

$$\chi(T) = \chi_p + \frac{C_{\mathrm{Curie}}}{T + \theta_W}.$$

We can see contrasting behaviors between the two different kinds of chemical substitutions. The reduction of T_N (or T_{peak}, T_{SG}) and θ_W is much faster in the case of Ru substitution for Ti, while the Zn substitution does not change C_{Curie} and χ_p. The effective moment remains to be approximately $1.95\mu_B$ even at $z=0.5$ and no contribution to the susceptibility from itinerant carriers is confirmed. These results mean that there is a strong correlation between the suppression of the magnitude of localized spins and the enhancement of the Pauli's paramagnetic susceptibility. In other words, the strong correlation between C_{Curie} and χ_p means that the localization-to-itinerant crossover of Cu^{2+} is the center player of magnetic and electronic properties of the present system.

IV. DISCUSSION

The heat-capacity measurements reveal a successive change of the magnetic ground states, which are not a simple blend of antiferromagnetic insulator and metal. It is no doubt that the various magnetic ground states are induced by a complicated interplay of localized spins and itinerant electrons driven by Ru substitutions. In Sec. IV, we will discuss first how the parent $CaCu_3Ti_4O_{12}$ acquire metallicity with increasing x and then discuss what is the origin of the T^2 proportional heat capacity for $x=0.5$.

A. Role of Ru substitution

As was discussed by Kobayashi *et al.*,[1] Ru substitution monotonically increases χ_p consistent with the gradual appearance of metallicity. The heat-capacity measurements reveal the corresponding monotonic evolution of γ as shown in Fig. 5(e). Since $CaCu_3(Ti_{4-x}Ru_x)O_{12}$ has an isotropic three-dimensional structure, we try to fit two points, $(x, \gamma)=(0,0)$ and (0.5, 0.0185), with a simple formula of $\gamma(x) \propto x^{-1/3}$, which is applicable to an initial stage of carrier doping to an isotropic band insulator such as Y-substituted $CaTiO_3$.[16] It is surprising that the $x^{-1/3}$ law looks valid up to $x=1.5$, which suggests a possible band filling from $x=0$ to 1.5. Several band-calculation studies predict an opening of finite gap in $CaCu_3Ti_4O_{12}$ even though the character of a conduction band has not been settled; Fagan *et al.*[17] concluded that a conduction band consists mainly of Cu and O antibonding level only, while Shiraki *et al.*[9] emphasized that Cu and Ti both contribute to a conduction band. What is important is that both calculations predict that the carrier is considered to itinerate on the Cu and O levels and thus the strong correlation between the evolution of DOS at E_F and the suppression of localization of Cu^{2+} spins seem to be reasonable.

However, we should also note that there are two factors that differentiate Ru-substituted $CaCu_3Ti_4O_{12}$ from Y-substituted $CaTiO_3$. One is that Ru substitution for Ti is an isovalent substitution as is emphasized by Kobayashi *et al.*[1] and the other is the difference of the parent insulators; $x=0$ should be regarded as a Mott insulator. We believe that the situation should be distinguished rigorously from the rigid-band picture as for the case of Y-substituted $CaTiO_3$, and more complicated change might be induced by the Ru substitution. In addition, the x dependence of χ_p does not exactly follow the $x^{-1/3}$ law in contrast to $\gamma(x)$ as is shown in Fig. 5(e). In order to clarify the novel insulator-to-metal crossover, a further study of doping dependence will be necessary, particularly at $0 \leq x \leq 0.5$.

In contrast to the evolution of χ_p and γ even at small x, resistivity remains highly insulating.[1] However, we believe that the evolution of γ does not necessarily mean the metallic conduction because the insulator-to-metal crossover in the present compound is dominated also by a formation of percolation path. Ramirez *et al.*[2] reported that a true metallic state is realized when x approaches 3. The extrapolation of the present $x^{-1/3}$ line gives approximately $\gamma = 0.04$ J mol^{-1} K^{-2} at $x=4$, which is less than half of the actual value, 0.084 J mol^{-1} K^{-2}. This suggests that the acquisition of metallic conduction is accomplished through at least two steps. We should call attention that one of the possible scenario has been already discussed in previous studies; at smaller x, metallic conduction is mainly dominated by a Cu-O-Ru network, while at larger x both Ru-O-Ru and Cu-O-Ru networks contribute.[1,2] How γ evolves with x observed in the present study looks consistent with these predictions. It is also interesting to see the Willson ratio of the $x=0.5$ and 1.5 compounds show a similar value to that of $x=4.0$ ($CaCu_3Ru_4O_{12}$), even though the metallic resistivity is not observed. This implies that the enhancement of carrier mass by Ru substitution always works regardless of the coherent conduction of carriers.

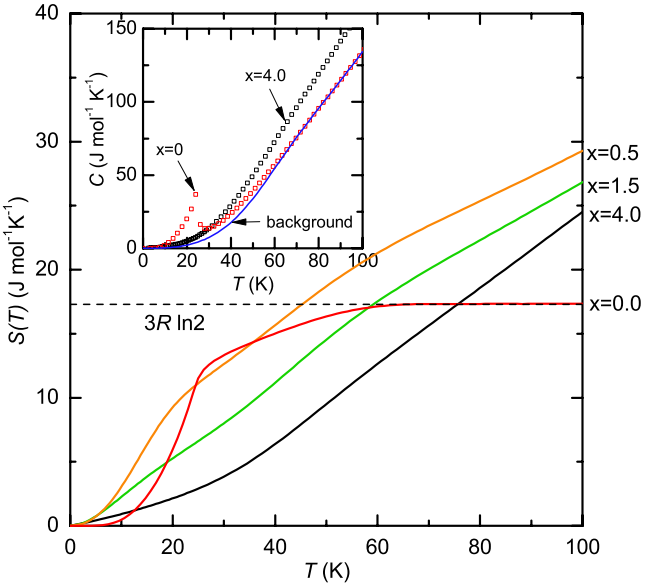

FIG. 6. (Color online) Temperature dependence of entropy of magnetoeletronic contribution after subtraction of appropriate background. For $x=0$, the $S(T)$ tends to saturate to the value of $3R$ ln 2 above $T=60$ K, indicating that the magnetic entropy is attributed to the localized $S=1/2$ spins on Cu^{2+} ions. For finite x (finite Ru substitution), such a saturation behavior is not observed, while the $S(T)$ keeps increasing toward $T=100$ K, implying that the Ru substitution gives additional degrees of freedom to the system. Inset shows the background of phonon contribution used for the estimation of entropy. Data for $x=0$ and $x=4.0$, which are used to evaluate the phonon contribution, are also shown.

For further understanding, we try to extract electronic and magnetic entropies. Figure 6 shows the x dependence of entropy estimated after the common background contribution is subtracted. In order to extract the whole change caused by the Ru substitution, we assume a common background which can be assigned as a phonon contribution of the $x=0$ compounds. Unfortunately the large amount of magnetic contribution overlaps to the low-T heat-capacity data for $x=0$, we borrow that for $x=4.0$ to evaluate the leading term of C_{ph}, $\beta_0 T^3$. Then we combine the data calculated from $\beta_{ph} T^3$ below 20 K and raw data above 60 K of the $x=0$ and then fit it using a polynomial function including only the odd-power term of T such as

$$C_{\text{bakground}} = \beta_0 T^3 + \beta_1 T^5 + \ldots + \beta_9 T^{21},$$

following to a popular method.[18] The result is shown as a solid line in the inset of Fig. 6, which is identical to the data of $x=0$ at $T \geq 60$ K and is parallel to those of $x=4.0$ at $T \leq 20$ K. The entropy $S(T)$ is then calculated by performing a numerical integration of C/T as a function of T as shown in Fig. 6. Since there is no itinerant carrier at $x=0$, the estimated entropy should be purely due to localized $S=1/2$ spins on Cu^{2+} ions. The entropy saturates above $T=60$ K at the value very close to $3R$ ln 2 (R: gas constant), which is consistent with the isolated $S=1/2$ spin picture. At the transition temperature, however, the entropy for $x=0$ does not reach the saturation value at T_N suggesting the remanent short-

range ordering and/or fluctuations above T_N. The estimation for $x=0$ is consistent with the entropy analysis by Ramirez *et al.*[2]

Rapid increase of the entropy is observed after Ru substitution. For $x=0.5$, the saturation behavior disappears completely and the entropy keeps increasing to $T=100$ K instead. This indicates that the Ru substitution glues additional entropy to the system. Since the contribution from the localized spins is believed to decrease monotonically with increasing x,[2] the present increase of the total entropy is likely due to itinerant carriers and/or Ru ions themselves. However, it is still an open question how the Ru^{4+} ions behave with surrounding Cu^{2+} and O^{2-} ions. The presence of strong hybridization of surrounding Cu^{2+} and O^{2-} suggests a formation of complicated electronic states that cannot be attributed to an individual ion.[19] The increase of additional entropy means that the extra degrees of freedom are added by Ru^{4+} ions through the strong hybridization to the Cu^{2+} levels. We believe that this hybridization is sufficient to create a finite DOS at E_F, but is not enough to allow the induced carrier to itinerate freely like an ordinary metal. We believe that this anomalous evolution of the entropy is a key to the full understanding of the insulator-to-metal crossover in $CaCu_3(Ti_{4-x}Ru_x)O_{12}$, and, for example, microscopic probe such as a STM will become a powerful tool to reveal the true role of Ru substitution.

B. Origin of T^2-proportional heat capacity at $x=0.5$

Next we focus on the origin of the T^2 dependence of the heat capacity appearing on the way of a transition from 3D AF-LRO to SG-like states. Based on textbook knowledge of metal, we usually assign the T-linear term to the contribution of itinerant electrons and the T^3 term to the contribution of phonons. However, there are no simple particles that automatically obey T^2 law and thus we should consider a more complicated situation to understand it. One possibility is a classical AF spin-wave excitation in a two-dimensional space. However, this is unlikely because the crystal structure remains isotropic and no indication of dimensional reduction by Ru substitution. Another possible situation is that the opening of finite gap in the excitation spectrum like a partially gapped superconductor such as d-wave high-T_c cuprate and p-wave Sr_2RuO_4 superconductors.[20–22] However, the T^2 behavior does not predominate over other temperature dependences in these compounds and it is almost impossible to directly observe T^2 behavior. One of the striking features of $CaCu_3Ti_{3.5}Ru_{0.5}O_{12}$ is that the dominant region of the T^2 law is spread widely, which implies that this T^2-proportional heat capacity is intrinsic, but not a consequence of phase segregation and/or phase mixture of AF-LRO ($x=0$) and SG ($x \geq 1.0$) phases.

Recently, several different classes of materials have been reported to show the T^2-proportional heat capacity in several spin-frustration compounds. Ramirez *et al.*[2] found that the heat capacity of Kagomé lattice compound $SrCr_9Ga_3O_{19}$ shows the T^2-proportional behavior.[23] While its magnetic susceptibility is typical for a spin-glass material, the T^2 dependence of the heat capacity challenges the SG scenario.[24]

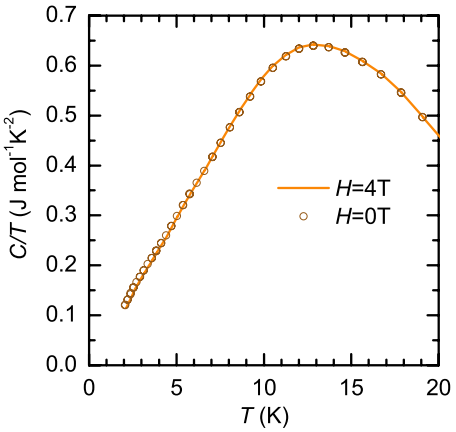

FIG. 7. (Color online) Heat-capacity data of $x=0.5$ sample measured at $H=0$ and 4 T.

They also found that the heat capacity of $SrCr_9Ga_3O_{19}$ does not depend on external magnetic field,[25] implying a presence of many-body singlet excitations in the low-energy excitation spectrum.[26] The magnetic field dependence of the heat capacity for $x=0.5$ is very weak, as shown in Fig. 7, which suggests a common feature to the T^2-proportional heat capacity. Similar T^2 behavior were also reported for the two-dimensional (2D) triangular lattice compound $NiGa_2S_4$,[27] in which only magnetic short-range order exists at the magnetic ground state. These compounds have no magnetic long-range order at the ground state, so that it should be distinguished from a classical AF spin-wave theory in two-dimensional state and the absence of long-range order looks similar to the $x=0.5$. Quite recently, however, this field-independent T^2-proportional heat capacity is explained qualitatively by spin-wave excitatons of the helical spin structure.[28]

These two compounds are, however, different from the Ru-substituted $CaCu_3Ti_4O_{12}$ in several points. One significant difference is the degree of frustration. $SrCr_9Ga_3O_{19}$ and $NiGa_2S_4$ have Kogomé and triangular lattices, respectively. Thus, localized spins located on these lattices feel strong geometrical frustration. In fact, the degree of frustration can be evaluated from the ratio of T_N and θ_W as $|\theta_W|/T_N=150$ for $SrCr_9Ga_3O_{19}$ (Ref. 23) and $|\theta_W|/T_N=8$ for $NiGa_2S_4$,[27] which are sufficiently large to expect the strong frustration. On the contrary, this ratio is small in the present case: $|\theta_W|/T_N=1.78$ at $x=0$ and $|\theta_W|/T_{peak}=1.79$ at $x=0.5$ implying that the influence of frustration is not dominant in $CaCu_3(Ti_{4-x}Ru_x)O_{12}$. Another difference is that the present T^2-dependent heat capacity appears only after carrier is induced in the parent insulator, while $SrCr_9Ga_3O_{19}$ and $NiGa_2S_4$ show their peculiar heat capacity without carrier doping. Thus, the situation is much more complicated in our case and we need to take the coupling between localized spins and doped holes into account.

The characteristics of Ru substitution is then summarized as follows: (1) Ru suppresses AF-LRO more rapidly than that expected by a dilution effect; (2) Ru creates a new magnetic ground state where heat capacity is proportional to T^2; (3) Ru suppresses the magnitude of effective moment of localized spins on Cu^{2+} ions; and (4) Ru adds itinerant carriers to the parent compound as indicated by resistivity,

thermopower,[1] and electronic specific heat. High-T_c cuprate superconductor $La_{2-x}Sr_xCuO_4$ gives a hint to understand the meaning of Ru substitution because the suppression of AF LRO in the parent La_2CuO_4 goes in a different way between two types of chemical substitution. Zn (or Mg) substitution for Cu simply reduces T_N while keeping AF LRO (Ref. 29) and completely disappears at $x_c \approx 41\%$ showing a good agreement with 2D percolation threshold.[30] Sr substitution for La shows a marked difference. In this case, Sr adds holes to the parent Mott insulator[31] and the suppression of AF LRO is much faster than that for the Zn substitution. The difference between the Ru- and Zn-substitution effects in $CaCu_3Ti_4O_{12}$ is very similar to the case of La_2CuO_4 and therefore they likely have common features. It is worth noting that the SG state emerges in $La_{2-x}Sr_xCuO_4$, which is understood to be resulting from bond frustration introduced by doped holes.[32] The central mystery of Ru-substituted $CaCu_3Ti_4O_{12}$ is that the similar change occurs without explicit chemical doping. Recently, detailed specific-heat measurement of slightly doped $La_{2-x}Sr_xCuO_4$ has been done, in which the electronic specific heat is found to start growing even from $x=0$.[33] This indicates the sensitivity of an AF-LRO of parent Mott insulating state to the doped carriers in common.

We should finally call readers' attention to the proposal of approximately T^2-proportional heat capacity for 2D graphene,[34] where the Fermi level is located close to the band-crossing point, and thus, the density of state becomes very small. This reminds us of the similarity to the present case of partially Ru-substituted $CaCu_3Ti_4O_{12}$, in which a small density of state at the Fermi level might be expected. It is thus interesting to compare the present T^2-proportional heat-capacity to a band structure of $CaCu_3(Ti_{3.5}Ru_{0.5})O_{12}$.

V. SUMMARY

In summary, we investigate the effect of Ru substitution for Ti on the ground-state properties of $CaCu_3Ti_4O_{12}$. We find that even a small amount of holes doped by Ru drastically suppresses the AF-LRO and induces a new magnetic ground state with peculiar thermodynamic properties. The observed T^2 law of the heat capacity indicates that the magnetic and electronic excitations are no longer independent from each other and resultingly demonstrates the complicated interplay between itinerant and localized electrons on Cu^{2+} ions. Although the microscopic origin of the T^2-proportional heat capacity has not been clarified yet, it is strongly suggestive that the present T^2 dependence of the heat capacity is one of the inherent features of the doped Mott insulator.

ACKNOWLEDGMENTS

We appreciate Y. Kato, S. Komiya, and S. Ono for valuable discussions and A. A. Taskin for critical reading.

*ichiro@criepi.denken.or.jp

[1] W. Kobayashi, I. Terasaki, J. Takeya, I. Tsukada, and Y. Ando, J. Phys. Soc. Jpn. **73**, 2373 (2004).
[2] A. P. Ramirez, G. Lawes, D. Li, and M. A. Subramanian, Solid State Commun. **131**, 251 (2004).
[3] M. A. Subramanian, D. Li, N. Duan, B. A. Reisner, and A. W. Sleight, J. Solid State Chem. **151**, 323 (2000).
[4] C. C. Homes, T. Vogt, S. M. Shapiro, S. Wakimoto, and A. P. Ramirez, Science **293**, 673 (2001).
[5] Y. J. Kim, S. Wakimoto, S. M. Shapiro, P. M. Gehring, and A. P. Ramirez, Solid State Commun. **121**, 625 (2002).
[6] A. Koitzsch, G. Blumberg, A. Gozar, B. Dennis, A. P. Ramirez, S. Trebst, and S. Wakimoto, Phys. Rev. B **65**, 052406 (2002).
[7] A. Krimmel, A. Günther, W. Kraetschmer, H. Dekinger, N. Büttgen, A. Loidl, S. G. Ebbinghaus, E.-W. Scheidt, and W. Scherer, Phys. Rev. B **78**, 165126 (2008).
[8] M. Fisher, Philos. Mag. **7**, 1731 (1962).
[9] H. Shiraki, T. Saito, T. Yamada, M. Tsujimoto, M. Azuma, H. Kurata, S. Isoda, M. Takano, and Y. Shimakawa, Phys. Rev. B **76**, 140403(R) (2007).
[10] See, for example, H. Aruga-Katori and A. Ito, J. Phys. Soc. Jpn. **63**, 3122 (1994).
[11] S. F. Edwards and P. W. Anderson, J. Phys. F: Met. Phys. **5**, 965 (1975).
[12] D. Sherrington and S. Kirkpatrick, Phys. Rev. Lett. **35**, 1792 (1975).
[13] R. Kubo, Phys. Rev. **87**, 568 (1952).
[14] D. Stauffer and A. Aharony, *Introduction to Percolation Theory*, Revised 2nd ed. (Taylor and Francis, Bristol, PA, 1994).
[15] A. B. Harris and S. Kirkpatrick, Phys. Rev. B **16**, 542 (1977).
[16] Y. Tokura, Y. Taguchi, Y. Moritomo, K. Kumagai, T. Suzuki, and Y. Iye, Phys. Rev. B **48**, 14063 (1993).
[17] S. B. Fagan, A. G. Souza Filho, A. P. Ayala, and J. Mendes Filho, Phys. Rev. B **72**, 014106 (2005).
[18] See, for example, Y. Ando, N. Miyamoto, K. Segawa, T. Kawata, and I. Terasaki, Phys. Rev. B **60**, 10580 (1999). This expansion is valid when energy dispersion of acoustic phonon is assumed to have the form of $\hbar\omega = c|\sin ka|$.
[19] H. Xiang, X. Liu, E. Zhao, J. Meng, and Z. Wu, Phys. Rev. B **76**, 155103 (2007).
[20] N. Momono and M. Ido, Physica C **264**, 311 (1996).
[21] K. A. Moler, D. L. Sisson, J. S. Urbach, M. R. Beasley, A. Kapitulnik, D. J. Baar, R. Liang, and W. N. Hardy, Phys. Rev. B **55**, 3954 (1997).
[22] S. Nishizaki, Y. Maeno, S. Farner, S. Ikeda, and T. Fujita, J. Phys. Soc. Jpn. **67**, 560 (1998).
[23] A. P. Ramirez, G. P. Espinosa, and A. S. Cooper, Phys. Rev. Lett. **64**, 2070 (1990).
[24] N. F. Mott, *The Metal-Insulator Transition* (Taylor and Francis, London, 1974).
[25] A. P. Ramirez, B. Hessen, and M. Winklemann, Phys. Rev. Lett. **84**, 2957 (2000).
[26] P. Sindzingre, G. Misguich, C. Lhuillier, B. Bernu, L. Pierre, Ch. Waldtmann, and H.-U. Everts, Phys. Rev. Lett. **84**, 2953 (2000).

[27] S. Nakatsuji, Y. Nambu, H. Tonomura, O. Sakai, S. Jonas, C. Broholm, H. Tsnuetsugu, Y. Qiu, and Y. Maeno, Science **309**, 1697 (2005).
[28] H. Yamaguchi, S. Kimura, M. Hagiwara, Y. Nambu, S. Nakatsuji, Y. Maeno, and K. Kindo, Phys. Rev. B **78**, 180404(R) (2008).
[29] K. Uchinokura, T. Ino, I. Terasaki, and I. Tsukada, Physica B **205**, 234 (1995).
[30] O. P. Vajk, P. K. Mang, M. Greven, P. M. Gehring, and J. W. Lynn, Science **295**, 1691 (2002).
[31] M. Hücker, V. Kataev, J. Pommer, J. Haraß, A. Hosni, C. Pflitsch, R. Gross, and B. Büchner, Phys. Rev. B **59**, R725 (1999).
[32] I. Ya. Korenblit, A. Aharony, and O. Entin-Wohlman, Phys. Rev. B **60**, R15017 (1999).
[33] S. Komiya and I. Tsukada, arXiv:0808.3671, J. Phys.: Conf. Ser. (to be published).
[34] See, for example, K. S. Yi, D. Kim, and K.-S. Park, Phys. Rev. B **76**, 115410 (2007).